

# Encapsulation of Nanoparticles Using Nitrilotriacetic Acid End-Functionalized Polystyrenes and Their Application for the Separation of Proteins

Mohammad Abdul Kadir, Su Jeong Kim, Eun-Ju Ha, Hong Y. Cho, Bong-Soo Kim, Donghyeuk Choi, Sun-Gu Lee, Bog G. Kim, Sang-Wook Kim, and Hyun-jong Paik\*

The use of nitrilotriacetic acid end-functionalized polystyrenes (NTA-PS) as a multifunctional nanocarrier for the aqueous dispersion of CdSe,  $\gamma$ -Fe<sub>2</sub>O<sub>3</sub> and gold nanoparticles (NPs) is described. When the amphiphilic end-functionalized polystyrenes and NPs are dissolved together in tetrahydrofuran, the addition of water causes the spontaneous formation of micellar aggregates, resulting in the successful encapsulation and aqueous dispersion of NPs. Transmission electron microscopy (TEM), scanning electron microscopy (SEM), photoluminescence (PL) spectroscopy, and vibrating sample magnetometer (VSM) are used to characterize the structure and properties of the NPs-containing micellar aggregates (nanocarrier). After complexation of Ni<sup>2+</sup> with NTA on the surface of the nanocarrier containing  $\gamma$ -Fe<sub>2</sub>O<sub>3</sub>, specific binding between Ni-NTA complex and histidine-tagged (His-tagged) proteins enables selective separation of His-tagged proteins using a magnet.

on hydrophobic interactions between the core-forming polymer chains. The process is concomitantly driven by a gain in entropy of the solvent molecules as the hydrophobic components withdraw from the aqueous media. The inherent immiscibility between different blocks and the competing thermodynamic effects give rise to spherical, lamellar, vesicular, rod-like, and gyroidal molecular architectures depending on the volume fraction, chemical composition, segmental interaction, and molecular weight of block copolymers.<sup>[2,3]</sup>

In recent years, polymeric micelles have been the subject of growing scientific interest.<sup>[4]</sup> Polymeric micelles have emerged as a novel promising colloidal carrier for the targeting of poorly water soluble drugs and nanoparticles (NPs).<sup>[5–7]</sup>

## 1. Introduction

Polymeric micelles are supramolecular self-assemblies of synthetic macromolecules where individual amphiphilic polymers aggregate together by noncovalent interactions.<sup>[1]</sup> The self-assembly of amphiphilic block copolymers in water is based

This ability to encapsulate molecules in nanocarriers opens the way towards diverse applications such as medical (drug delivery),<sup>[6]</sup> molecular imaging<sup>[8]</sup> and catalysis (enzyme entrapment).<sup>[9]</sup> Therefore, it has attracted the attentions to work with the polymeric micelles with encapsulated NPs in the core.<sup>[10–12]</sup> Over the past several years, researchers have witnessed the development of nanoparticulate system in drug delivery<sup>[5,6,13,14]</sup> and molecular imaging applications.<sup>[8,15]</sup> Polymeric micelle that is assembled NPs from amphiphilic block copolymers easily provides stable core-shell architecture as a nanocarrier and hydrophilic shell allows particle to stabilize in the aqueous solution. In the other words, they can impart an aqueous dispersive property to hydrophobic NPs including metals, metal oxides and semiconductors (quantum dots, QDs).

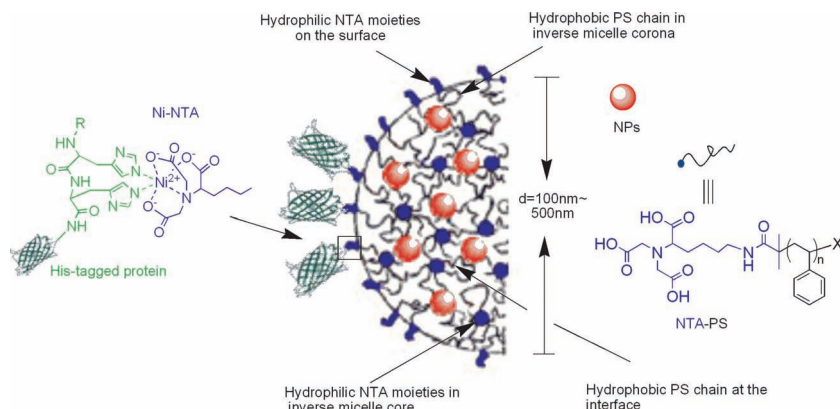
Water-dispersive multifunctional combination of NPs has potential applications, for example, QDs for imaging and magnetic NPs for separation of biomolecules and biomedical application.<sup>[16–24]</sup> Block copolymer micelles containing NPs have been reported by Taton group and others, respectively.<sup>[10,25–32]</sup> In another study, Taton and co-workers have shown that polystyrene-*block*-polyacrylate copolymer micelles can be used with combinations of magnetic NPs through the several steps and they could prove a magnetomicelle could be used as a support for recycling of biocatalyst and bioseparation by attaching iminodiacetic acid (IDA) to the micelle surface.<sup>[33]</sup>

M. A. Kadir, S. J. Kim, Dr. E.-J. Ha, H. Y. Cho,  
Dr. B.-S. Kim, Prof. H.-j. Paik  
Department of Polymer Science and Engineering  
Pusan National University  
San 30 Jangjeon 2-dong Geumjeong-gu,  
San 609-735, Korea  
E-mail: hpaik@pusan.ac.kr



D. Choi, Prof. S.-W. Kim  
Department of Molecular Science and Technology  
Ajou University  
San 5 Wonchon-dong, Youngtong-gu, Suwon 442-749, Korea  
Prof. S.-G. Lee  
Department of Chemical Engineering  
Pusan National University  
San 30 Jangjeon 2-dong Geumjeong-gu, Busan 609-735, Korea  
Prof. B. G. Kim  
Department of Physics  
Pusan National University  
San 30 Jangjeon 2-dong Geumjeong-gu, Busan 609-735, Korea

DOI: 10.1002/adfm.201200849



**Scheme 1.** Multifunctional polymeric nanocarriers for protein separations.

While majorities of encapsulation works were carried out by using amphiphilic block copolymers, no attention was given to the use of end-functionalized amphiphilic homopolymers. The presence of inherent functional group in end-functionalized polymer reduces the synthetic steps after encapsulation of NPs to produce functional nanomaterials. In addition, reactive end-groups allow precise incorporation of one entity at a defined position on the polymer and thus provide superior control and specificity. Therefore, the use of end-functionalized amphiphilic homopolymer for encapsulation of various NPs could be a useful technique for their further applications depending on the functional group introduced at the chain end.

Here we report the use of end-functionalized amphiphilic homopolymer to encapsulate various NPs into the micellar aggregates. A new multifunctional polymeric nanocarrier is developed for aqueous dispersion of CdSe,  $\gamma\text{-Fe}_2\text{O}_3$  and gold NPs using nitrilotriacetic acid end-functionalized polystyrenes.<sup>[34]</sup> As nitrilotriacetic acid (NTA) complexed with  $\text{Ni}^{2+}$  is well-known to have strong interaction with a sequence of histidine residues of biomolecules,<sup>[35–46]</sup> micellar aggregates containing magnetic NPs (e.g.,  $\gamma\text{-Fe}_2\text{O}_3$ ) inside (nanocarriers) and having NTA functionality on the surface could be used for bioconjugation and bioseparation (Scheme 1).

## 2. Results and Discussion

### 2.1. Encapsulation of Nanoparticles

NTA is a tetradentate ligand which occupies four of the six binding sites of  $\text{Ni}^{2+}$ , leaving two free sites for histidine-tagged proteins (His-tagged proteins) to bind. The  $\text{Ni}^{2+}$  complexation with a histidine is a fast and reversible reaction. A competitor ligand, such as imidazole can displace the His-tagged proteins. In our previous study, we reported

synthesis of  $\alpha$ -(nitrilotriacetic acid)-end-functionalized polystyrenes ( $\alpha$ -NTA-PS) by atom transfer radical polymerization (ATRP) using NTA-functionalized initiator and by taking advantages of NTA's hydrophilic nature and its chemistry as mentioned, we were able to produce micellar aggregates in aqueous phase, which could bind (six histidine-tagged green fluorescent proteins) His<sub>6</sub>-GFP on the surface of micellar aggregates specifically through NTA- $\text{Ni}^{2+}$ /histidine (His) interaction.<sup>[47]</sup>

Among many nanoparticulate systems, self-assembled NPs from amphiphilic polymers, provide a unique core-shell architecture wherein the hydrophobic core serves as a natural carrier environment for hydrophobic NPs and the hydrophilic shell allows particle stabilization in the aqueous solution. When QDs were dissolved together with  $\alpha$ -NTA-PS in THF, the slow addition of water and the removal of THF by evaporation caused the encapsulation and aqueous dispersion of QDs. The transmission electron microscopy (TEM) and scanning electron microscopy (SEM) images of pure micellar aggregates (without NPs) are shown in Figure 1a,b, respectively. The successful encapsulation of QDs inside the micellar aggregates was evidenced by TEM

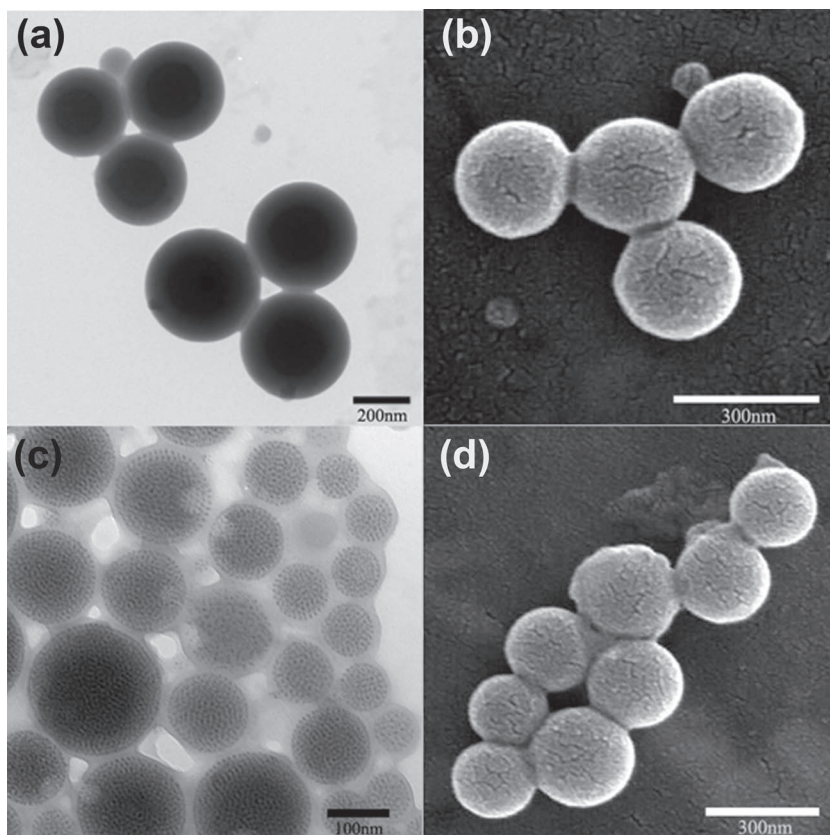


**Figure 1.** TEM and SEM images of the micellar aggregates from the  $\alpha$ -(NTA)-polystyrenes. Pure micellar aggregates: a) TEM image and b) SEM image. Micellar aggregates containing CdSe QDs: c) TEM image and d) SEM image. SEM samples were coated with Pt layers by the ion sputter.



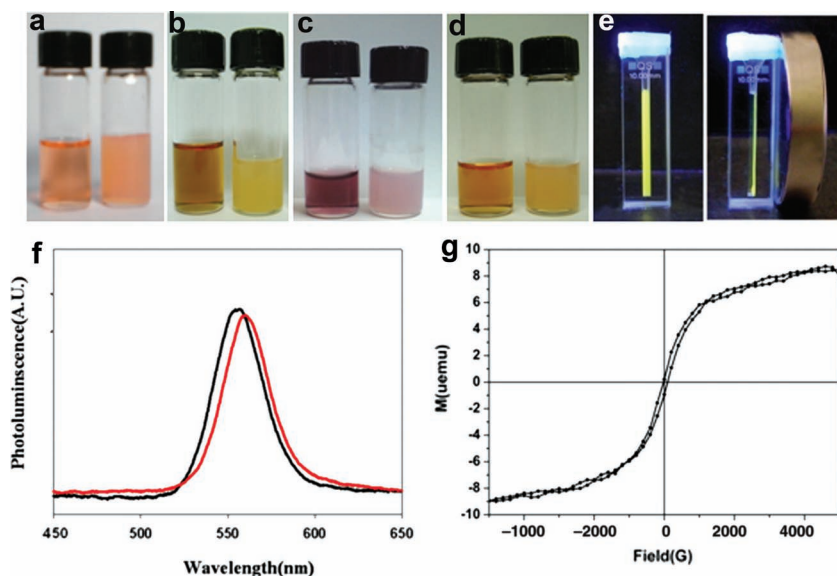


**Figure 2.** The digital photographs of original NPs in THF (left) and the solution of micellar aggregates containing NPs in water (right) and their properties. The photographs show a) CdSe QDs, b)  $\gamma\text{-Fe}_2\text{O}_3$  NPs, c) Au NPs, and the mixture of CdSe QDs and  $\gamma\text{-Fe}_2\text{O}_3$  NPs under d) room light and e) UV light. f) Photoluminescence spectra of CdSe QDs in THF (black) and encapsulated QDs in micellar aggregates (red). g) VSM hysteresis loop of  $\gamma\text{-Fe}_2\text{O}_3$  NPs in micellar aggregates.

observation (Figure 1c). The SEM image of QDs-encapsulated micellar aggregates is shown in Figure 1d, which are also spherical and similar in size comparable to that of pure micellar aggregates (Figure 1b). The presence of QDs inside the micellar aggregates was also confirmed by the fluorescent optical microscopy (S-Figure 4, Supporting Information). Besides, the solution became translucent due to formation of micellar aggregates and QDs did not precipitate because of their successful encapsulation inside the micellar aggregates (Figure 2a, right). The emission peak of QDs in the micellar aggregates was similar to that in the organic solvent (Figure 2f).

To explore the generality of the approach, similar encapsulation experiments were also carried out using other NPs including magnetic  $\gamma\text{-Fe}_2\text{O}_3$  and metallic gold. TEM studies revealed that the NPs were encapsulated in the micellar aggregates. The TEM images of  $\gamma\text{-Fe}_2\text{O}_3$  ( $\approx 8\text{--}9$  nm) NPs and their encapsulated micellar aggregates are shown in Figure 3a,b, respectively. The solution also became translucent due to formation of micellar aggregates and  $\gamma\text{-Fe}_2\text{O}_3$  NPs did not precipitate because of their successful encapsulation inside the micellar aggregates (Figure 2b, right). The magnetic properties of  $\gamma\text{-Fe}_2\text{O}_3$  NPs in the micellar aggregates were measured by vibrating sample magnetometers (VSM) in water. The field-dependent magnetization loop of the NPs (Figure 2g) suggested that they had superparamagnetic properties, which were more appropriate for magnetic separation than ferromagnetism because the magnetic properties disappeared when the field removed. Metallic gold NPs (Figure 3e) were also encapsulated following the similar procedure (see Figure 3f and Figure 2c, right).

To make multifunctional assemblies,  $\gamma\text{-Fe}_2\text{O}_3$  NPs (Figure 3a) and QDs (Figure 3c) were mixed together and encapsulated in the micellar aggregates simultaneously. The successful

encapsulation of two types of NPs inside the micellar aggregates was evidenced by TEM observation (Figure 3d). The solution also became translucent due to formation of micellar aggregates and no precipitation was occurred due to successful encapsulation of both type of NPs inside the micellar aggregates (Figure 2d, right). The concurrent existence of fluorescence and magnetic properties in the resulting solution under UV light was the evidence of the new combination of magnetization and fluorescence using amphiphilic polymers (Figure 2e, right).

The NTA functional group has been well studied for their capability to form complex with  $\text{Ni}^{2+}$  that can bind histidine groups of biomolecules. Therefore, the complexation of  $\text{Ni}^{2+}$  with NTA on the surface of the NPs-containing micellar aggregates was further studied. An aqueous solution of  $\text{NiCl}_2$  was dissolved in an aqueous suspension of nanocarriers containing NPs. After stirring for 2 days, the excess  $\text{Ni}^{2+}$  was removed by dialysis. The successful complexation of  $\text{Ni}^{2+}$  with NTA on the surface of

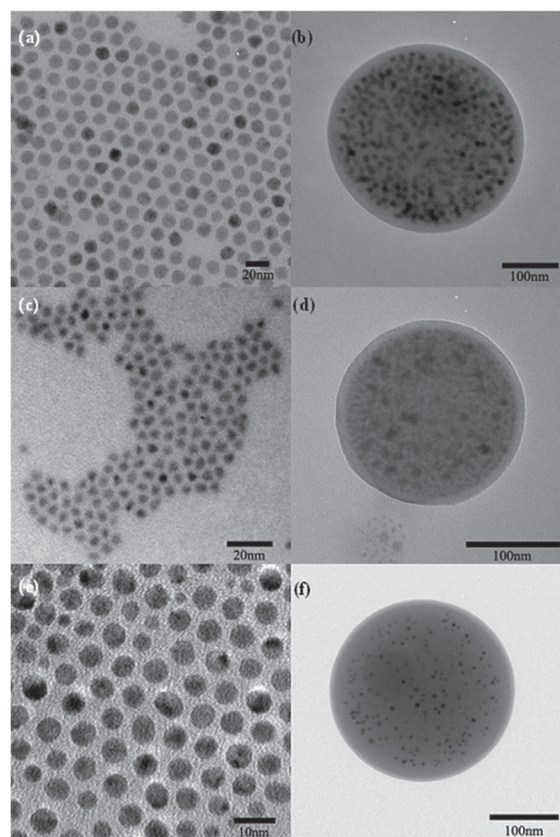


**Figure 3.** TEM images of NPs and micellar aggregates from the  $\alpha$ -(NTA)-polystyrenes. a) TEM image of the  $\gamma\text{-Fe}_2\text{O}_3$  NPs. b) TEM image of the micellar aggregate containing  $\gamma\text{-Fe}_2\text{O}_3$  NPs. c) TEM image of CdSe QDs. d) TEM image of the micellar aggregate containing the mixture of CdSe QDs and  $\gamma\text{-Fe}_2\text{O}_3$  NPs. e) TEM image of the Au NPs. f) TEM image of the micellar aggregate containing Au NPs.

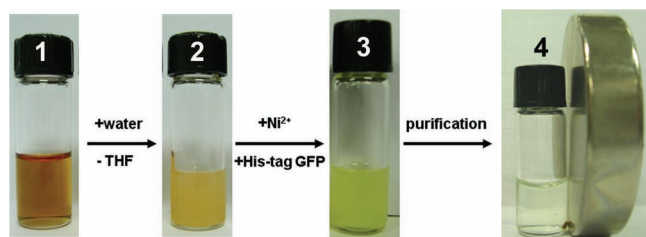


**Figure 4.** Preparation of nanocarrier and separation of His-tagged GFP using magnetic attraction.

the NPs-containing micellar aggregates was confirmed by the signal of  $\text{Ni}^{2+}$  in SEM/EDX (energy dispersive X-ray fluorescence) analysis (S-Figure 5, Supporting Information). The formation of  $\text{Ni}^{2+}$ -NTA complex on the surface of the nanocarrier opened the doors for bioconjugation and bioseparation of His-tagged proteins. We demonstrated the smart, selective and efficient separation of His-tagged proteins using the nanocarrier containing  $\gamma\text{-Fe}_2\text{O}_3$  NPs.

## 2.2. Separation of Proteins

The successful encapsulation of magnetic NPs and the complexation of  $\text{Ni}^{2+}$  with NTA on the surface of the nanocarrier offered the possibility of protein separation. The preparation of magnetic NPs-containing nanocarriers and the separation of His-tagged GFP are shown in **Figure 4**. First,  $\gamma\text{-Fe}_2\text{O}_3$  NPs and  $\alpha$ -NTA-PS were dissolved together in THF. Second, the slow addition of water and the removal of THF by evaporation caused the formation nanocarriers. Then, after the complexation of  $\text{Ni}^{2+}$  with NTA on the surface of the nanocarrier, His-tagged GFP was added to the solution. Finally, His-tagged GFP bound nanocarriers were attracted to the side of a vial using a magnet. The change of color of solution in each stages and the use of a magnet at the final stage, indicated the effectiveness and simplicity of our developed method for protein separation.

As shown in **Figure 5a–c**, fluorescent imaging also confirmed the efficient binding of the His-tagged GFP on the surface of the nanocarrier through the interaction between the  $\text{Ni}^{2+}$  and His-tagged. The fluorescence emission intensity of residual solution, i.e., the fluorescence emission intensity of free His-tagged GFP, which did not bind with micellar aggregates after separation from binding protein (with micellar aggregates) by magnet attraction was 10%, indicating the binding of 90% His-tagged GFP on the surface of nanocarriers. When concentrated imidazole solution was added to the nanocarriers containing His-tagged GFP on the surface, it

caused the release of His-tagged GFP and the fluorescence emission intensity of released His-tagged GFP was 41% (**Figure 5d**). While His-tagged GFP was separating using nanocarrier containing magnetic NPs, untagged protein, PE-Cy5 IgG1 (PE-Cy5 labeled immunoglobulin G1), had little interaction with NTA moiety. The fluorescence emission spectrum of the **Figure 5e** showed only 29% decreasing of fluorescence intensity in the residual solution. We also purified the His-tagged GFP from cell lysate using nanocarriers containing  $\gamma\text{-Fe}_2\text{O}_3$  NPs and the purity was confirmed by SDS-PAGE (sodium dodecyl sulfate-polyacrylamide gel electrophoresis) analysis (**Figure 5f**).

In a control experiment, we used the mixture of two proteins, His-tagged GFP and untagged-normal mouse IgG1. We were able to separate His-tagged GFP from the mixture of proteins using nanocarriers containing  $\gamma\text{-Fe}_2\text{O}_3$  NPs successfully, as was confirmed by fluorescent imaging and changing of emission intensity. These results also confirmed that the purification was achieved through the specific interactions between histidine and nickel.

## 3. Conclusions

We have developed a simple method for encapsulation of NPs for aqueous dispersion and selective separation of His-tagged proteins using NTA-end-functionalized polystyrenes. The generality of encapsulation method was demonstrated by incorporating

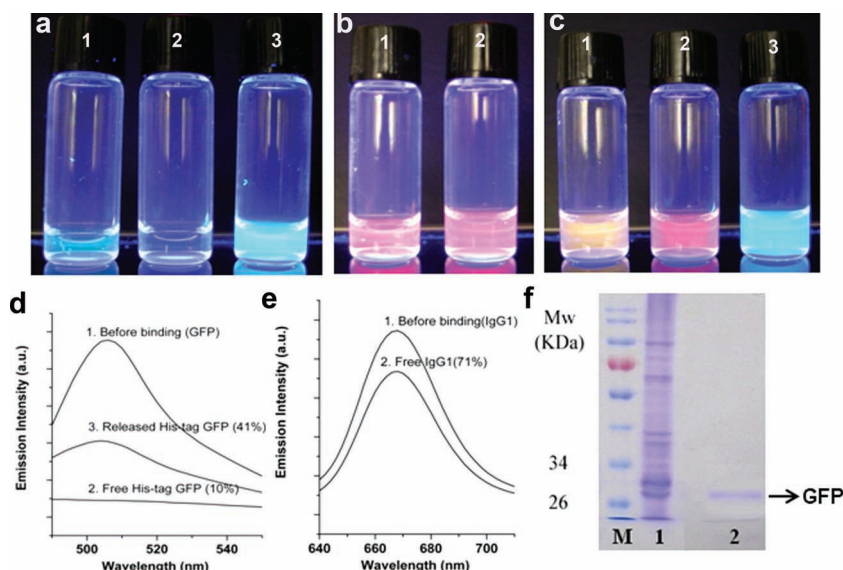
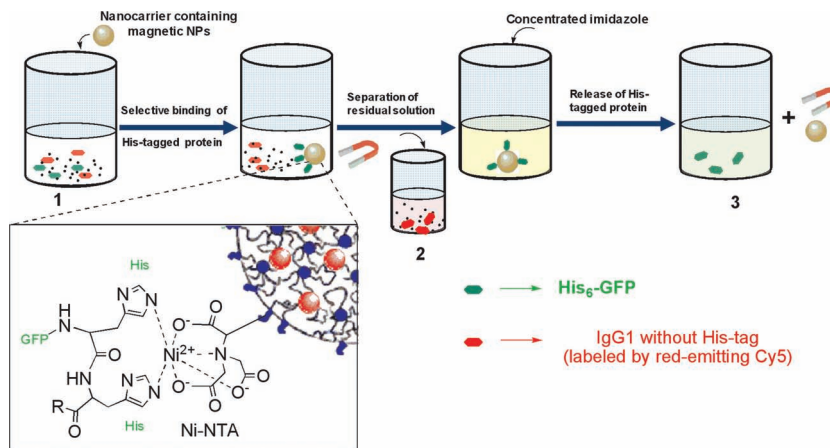


**Figure 5.** a) Fluorescent images from the solutions of His-tagged GFP: His-tagged GFP (1), residual solution after binding (free His-tagged GFP) (2), and after protein release with 250 mM imidazole solution (3). b) Normal mouse IgG1 conjugated by PE-Cy5: normal mouse IgG1 (1) and residual protein solution after binding (2). c) Fluorescent images from the solutions of mixture-protein (His-tagged GFP and IgG1) (1), residual protein after interaction with nanocarriers (2), and after release with 250 mM imidazole solution (3). d) Photoluminescence (PL) spectra of GFP: before binding with nanocarrier (free His-tagged GFP) (2), and after release with 250 mM imidazole solution (3). e) Photoluminescence (PL) spectra of IgG1: before binding (1) and residual solution after binding with nanocarrier (free IgG1) (2). f) SDS-PAGE (12% acrylamide gel) analysis of the cell lysate (lane 1) and after protein release with 250 mM imidazole (lane 2), lane M, molecular weight markers.



semiconductor, magnetic and metal NPs in the nanocarriers. The complexation of  $\text{Ni}^{2+}$  with NTA on the surface of nanocarriers containing magnetic NPs ( $\gamma\text{-Fe}_2\text{O}_3$ ) has opened the doors for biconjugation as well as selective and smart separation of His-tagged proteins from the mixture of proteins and cell lysate using a magnet. Because of the extensive usage of His-tagged proteins in biological research, this system will be a useful alternative for manipulating His-tagged proteins. We believe that our encapsulation method could be a general approach for end-functionalized amphiphilic homopolymers and nanocarrier of NTA-end-functionalized homopolymer can be further utilized in particular for recycling of expensive enzymes for catalysis.



**Scheme 2.** Separation of His-tagged protein.

## 4. Experimental Section

**Materials:** Styrene (Junsei, 99.5%) was purified by vacuum distillation over  $\text{CaH}_2$ .  $\text{Cu}(\text{I})\text{Cl}$  (Aldrich, 98%) were purified by stirring with glacial acetic acid followed by filtering and washing the resulting solids with ethanol ( $\times 3$ ) and diethyl ether ( $\times 2$ ), respectively.  $N,N,N',N'',N''$ -pentamethyldiethylenetriamine (PMDETA) (Aldrich, 98%) was purified by vacuum distillation. 4,4'-di(5-nonyl)-2,2'-bipyridine (dNbpy) (97%), *tert*-butyl bromoacetate (98%), 2,2'-dipyridyl (bpy) (99%+), palladium (10 wt% activated carbon), and 2-bromoisobutyl bromide (98%) were purchased from Aldrich and used as received. H-Lysine(Z)-OtBu-HCl was used as received (Bachem, 99%+).  $N,N$ -bis[(*tert*-butoxycarbonyl)-methyl]-L-lysine *tert*-butyl ester was synthesized by following reported procedure.<sup>[48]</sup> Tetrahydrofuran (THF, 100%) and water ( $\text{H}_2\text{O}$ ) was BAKER ANALYZED HPLC Reagent. Normal mouse IgG1 conjugated by PE-Cy5 were purchased from Santa Cruz Biotechnology.

**Measurements:** Molecular weight ( $M_n$ ) and molecular weight distribution ( $M_w/M_n$ ) were determined using gel permeation chromatography (GPC), which was pre-calibrated with polystyrene standards. GPC was equipped with Agilent 1100 pump, RID detector, and PSS SDV ( $5\ \mu\text{m}$ ,  $10^5$ ,  $10^3$ ,  $10^2\ \text{\AA}$   $8.0 \times 300.0\ \text{mm}$ ) columns. Monomer conversion was determined by HP 5890 gas chromatography, equipped with HP101 column (Methyl Silicone Fluid,  $25\ \text{m} \times 0.32\ \text{mm} \times 0.3\ \mu\text{m}$ ).  $^1\text{H}$  NMR spectra were obtained using Varian Unity Plus 300 or Inova 500 FT-NMR spectrometers. Transmission electron microscopy (TEM) and scanning electron microscopy (SEM) images were obtained on a Hitachi H-7600 instrument at 100 kV and on a Hitachi S-4200, respectively. Energy dispersive X-ray fluorescence analysis (EDX, Horiba/EX-250) results were obtained by Hitachi/E-1030 ion sputter with Nikon/SMZ-U stereomicroscope. TEM samples were prepared by dipping a TEM grid (carbon coated grid) into respective solutions. SEM/EDX samples were prepared by dropping solution onto the silicon wafer. Extra solution was blotted with filter paper and dried for 12 h at room temperature. The hysteresis loop was obtained on vibrating sample magnetometer (VSM) Model 7407 LakeShore. The photoluminescence (PL) spectra were recorded using an Ocean Optics HR4000CG Composite-grating spectrophotometer with an excitation wavelength of 395 nm (for GFP) and 500 nm (for PE-Cy5 labeled IgG1).

**Preparation of  $\alpha$ -Nitrilotriacetic Acid End-Functionalized Polystyrenes:**  $\alpha$ -Nitrilotriacetic acid end-functionalized polystyrene ( $\alpha$ -NTA-PS) was prepared by atom transfer radical polymerization (ATRP) by using NTA functionalized initiator according to our previous reported procedure<sup>[47]</sup> unless stated otherwise (see Supporting Information for experimental part and characterization of polymer).

**Preparation of Nanoparticles (NPs):** Synthesis of CdSe QDs and  $\gamma\text{-Fe}_2\text{O}_3$  NPs are included in the Supporting Information. Au NPs were prepared by adding  $\text{Au}(\text{acetate})_3$  (30 mg, 0.08 mmol) to the degassed

solution of oleic acid (70.5 mg, 0.25 mmol), oleylamine (64.08 mg, 0.24 mmol) and octadecene (8 mL). The solution was slowly heated up ( $0.5\ ^\circ\text{C}/\text{min}$ ) to  $110\ ^\circ\text{C}$  and then cooled to room temperature. The final Au NPs were weighed by removing solvent and dispersed into dried THF with a known concentration.

**Encapsulation of Nanoparticles (NPs):** NPs solutions (CdSe,  $\gamma\text{-Fe}_2\text{O}_3$ , Au) were prepared using dried THF.  $\alpha$ -NTA-PS (1 mg,  $M_n$  (GPC) = 4700) was dissolved in desired NPs solution (1 mL) and then water (1 mL, BAKER ANALYZED HPLC Reagent) was added slowly to the mixture under rapid stirring. The resulted mixture was kept at  $60\ ^\circ\text{C}$  under stirring to remove THF from the mixture for 3 h (see Supporting Information for details).

**Nickel Complexation of Nanocarriers Containing NPs:** An aqueous solution of  $\text{NiCl}_2$  (1 mL, 1 mg/mL) was added to aqueous solution of nanocarriers (1.5 mL) containing NPs. The mixture was kept stirring for 1 day and then dialyzed with a cellulose ester membrane bag (Spectra/Por, molar mass cut off: 2000) against water to remove the excess nickel. The dialyzing water was changed three times for two days.

**Expression and Purification of His<sub>6</sub>-GFP:** *E. coli* BL21 (DE3) harboring the pET-GFPmut3.1 expressing GFPmut3.1<sup>[49]</sup> tagged with hexahistidine at its N-terminus was grown to OD<sub>600</sub> of 0.6 at  $37\ ^\circ\text{C}$  in Luria Bertani (LB, 100 mL) medium containing 100  $\mu\text{g}/\text{mL}$  of ampicillin, induced with 0.05 mM isopropyl  $\beta$ -D-thiogalactopyranoside (IPTG) for 6 h at  $20\ ^\circ\text{C}$ , and pelleted. Cells were lysed by using BugBuster protein extraction kit (Novagen). Briefly, collected cell pellet was resuspended in lysis buffer (5 mL), incubated at room temperature for 10 min, and centrifuged for 20 min at 9000 g and  $4\ ^\circ\text{C}$ . After the extracts was incubated with Ni-NTA HisBind Resin (Novagen, 5 mg) for 3 h at  $4\ ^\circ\text{C}$ , the resin was loaded into column, washed with washing buffer ( $2 \times 4\ \text{mL}$ , 50 mM phosphate buffer, pH 8.0; 300 mM NaCl; 20 mM imidazole), and the His<sub>6</sub>-GFP was eluted with elution buffer (1 mL, 50 mM phosphate buffer, pH 8.0; 300 mM NaCl; 250 mM imidazole). Imidazole in the eluted solution was removed by Diafiltration (Millipore). The protein fractions were analyzed by SDS-PAGE (12% acrylamide gel), showing that the purity of purified His<sub>6</sub>-GFP was more than 95%.

**Separation of Protein:** The general procedure of the separation of protein using Ni-NTA-decorated multifunctional nanocarrier containing magnetic NPs ( $\gamma\text{-Fe}_2\text{O}_3$ ) is schematically illustrated in **Scheme 2**. First, His<sub>6</sub>-GFP (1  $\mu\text{L}$ , 7  $\mu\text{g}/\mu\text{L}$ ) and the solution of nanocarriers containing  $\gamma\text{-Fe}_2\text{O}_3$  NPs (in phosphate buffer, pH 8.0, 300  $\mu\text{L}$ ) were mixed together and the resulted mixture was shaken for 1 h at room temperature. Second, the separation of the residual protein solution from the protein bound nanocarriers was performed using a magnet by attracting nanocarriers to the wall of the vial. Third, to release the His<sub>6</sub>-GFP from the surface of nanocarriers, a concentrated imidazole solution (250 mM) was added

to the solution of protein binded nanocarriers and also shaken for 1 h at room temperature. Finally, the nanocarriers were retrieved from the imidazole solution by applying a magnet. A control experiment was also performed following the similar procedure; but instead of His<sub>6</sub>-GFP, we used the mixture of two proteins, His<sub>6</sub>-GFP and normal mouse IgG1 without His-tagged and labeled by red-emitting Cy5 (200  $\mu$ L). Similar procedure was also followed to purify His-tagged GFP from a cell lysate.

## Supporting Information

Supporting Information is available from the Wiley Online Library or from the author.

## Acknowledgements

This work was supported by the Active Polymer Center for Pattern Integration (R11-2007-050-02002-0) and WCU (World Class University) program (R33-10035-0) through the National Research Foundation (NRF) grant funded by the Korea government (MEST).

Received: March 26, 2012

Revised: May 9, 2012

Published online: June 8, 2012

- [1] H. Ringsdorf, B. Schlarb, J. Venzmer, *Angew. Chem. Int. Ed.* **1988**, 27, 113.
- [2] L. Zhang, A. Eisenberg, *Science* **1995**, 268, 1728.
- [3] J. Rodríguez-Hernández, F. Chécot, Y. Gnanou, S. Lecommandoux, *Prog. Polym. Sci.* **2005**, 30, 691.
- [4] X. He, F. Schmid, *Phys. Rev. Lett.* **2008**, 100, 137802.
- [5] S. R. Croy, G. S. Kwon, *Curr. Pharm. Des.* **2006**, 12, 4669.
- [6] K. Kataoka, A. Harada, Y. Nagasaki, *Adv. Drug Delivery Rev.* **2001**, 47, 113.
- [7] H. Zhao, E. P. Douglas, B. S. Harrison, K. S. Schanze, *Langmuir* **2001**, 17, 8428.
- [8] J. K. Oh, *Soft Matter* **2011**, 7, 5096.
- [9] M. Mureseanu, A. Galarneau, G. Renard, F. Fajula, *Langmuir* **2005**, 21, 4648.
- [10] B.-S. Kim, J.-M. Qiu, J.-P. Wang, T. A. Taton, *Nano Lett.* **2005**, 5, 1987.
- [11] C. Giacomelli, V. Schmidt, R. Borsali, *Langmuir* **2007**, 23, 6947.
- [12] M. E. Gindy, A. Z. Panagiotopoulos, R. K. Prud'homme, *Langmuir* **2008**, 24, 83.
- [13] R. Savić, A. Eisenberg, D. Maysinger, *J. Drug Targeting* **2006**, 14, 343.
- [14] K. Miyata, R. J. Christie, K. Kataoka, *React. Funct. Polym.* **2011**, 71, 227.
- [15] J.-H. Kim, K. Park, H. Y. Nam, S. Lee, K. Kim, I. C. Kwon, *Prog. Polym. Sci.* **2007**, 32, 1031.
- [16] M. Bruchez Jr., M. Moronne, P. Gin, S. Weiss, A. P. Alivisatos, *Science* **1998**, 281, 2013.
- [17] J. K. Jaiswal, H. Mattoussi, J. M. Mauro, S. M. Simon, *Nat. Biotechnol.* **2003**, 21, 47.
- [18] W. J. Parak, D. Gerion, T. Pellegrino, D. Zanchet, C. Micheel, S. C. Williams, R. Boudreau, M. A. Le Gros, C. A. Larabell, A. P. Alivisatos, *Nanotechnology* **2003**, 14, R15.
- [19] I. L. Medintz, H. T. Uyeda, E. R. Goldman, H. Mattoussi, *Nat. Mater.* **2005**, 4, 435.
- [20] D. K. Yi, S. T. Selvan, S. S. Lee, G. C. Papaefthymiou, D. Kundaliya, J. Y. Ying, *J. Am. Chem. Soc.* **2005**, 127, 4990.
- [21] D. Wang, J. He, N. Rosenzweig, Z. Rosenzweig, *Nano Lett.* **2004**, 4, 409.
- [22] X. Michalec, F. F. Pinaud, L. A. Bentolila, J. M. Tsay, S. Doose, J. J. Li, G. Sundaresan, A. M. Wu, S. S. Gambhir, S. Weiss, *Science* **2005**, 307, 538.
- [23] I. S. Lee, N. Lee, J. Park, B. H. Kim, Y.-W. Yi, T. Kim, T. K. Kim, I. H. Lee, S. R. Paik, T. Hyeon, *J. Am. Chem. Soc.* **2006**, 128, 10658.
- [24] J. K. Oh, J. M. Park, *Prog. Polym. Sci.* **2011**, 36, 168.
- [25] Y. Kang, T. A. Taton, *Angew. Chem. Int. Ed.* **2005**, 44, 409.
- [26] Y. Kang, T. A. Taton, *Macromolecules* **2005**, 38, 6115.
- [27] B.-S. Kim, T. A. Taton, *Langmuir* **2007**, 23, 2198.
- [28] R. J. Hickey, A. S. Haynes, J. M. Kikkawa, S.-J. Park, *J. Am. Chem. Soc.* **2011**, 133, 1517.
- [29] B. L. Sanchez-Gaytan, S. Li, A. C. Kamps, R. J. Hickey, N. Clarke, M. Fryd, B. B. Wayland, S.-J. Park, *J. Phys. Chem. C* **2011**, 115, 7836.
- [30] A. C. Kamps, B. L. Sanchez-Gaytan, R. J. Hickey, N. Clarke, M. Fryd, S.-J. Park, *Langmuir* **2010**, 26, 14345.
- [31] J. Pyun, *Polym. Rev.* **2007**, 47, 231.
- [32] Y. Liu, X. Wang, *Polym. Chem.* **2011**, 2, 2741.
- [33] A. R. Herdt, B.-S. Kim, T. A. Taton, *Bioconjugate Chem.* **2006**, 18, 183.
- [34] M. A. Kadir, H. Y. Cho, B.-S. Kim, Y.-R. Kim, S.-G. Lee, U. Jeong, H.-j. Paik, in *Progress in Controlled Radical Polymerization: Materials and Applications*, Vol. 1101, (Eds: K. Matyjaszewski, B. S. Sumerlin, N. V. Tsarevsky), American Chemical Society, Washington, DC **2012**, Ch. 20.
- [35] B. R. Griffith, B. L. Allen, A. C. Rapraeger, L. L. Kiessling, *J. Am. Chem. Soc.* **2004**, 126, 1608.
- [36] T. Yu, Q. Wang, D. S. Johnson, M. D. Wang, C. K. Ober, *Adv. Funct. Mater.* **2005**, 15, 1303.
- [37] J. Porath, J. A. N. Carlsson, I. Olsson, G. Belfrage, *Nature* **1975**, 258, 598.
- [38] L. R. Paborsky, K. E. Dunn, C. S. Gibbs, J. P. Dougherty, *Anal. Biochem.* **1996**, 234, 60.
- [39] J. E. Gautrot, W. T. S. Huck, M. Welch, M. Ramstedt, *ACS Appl. Mater. Interfaces* **2010**, 2, 193.
- [40] E. K. M. Ueda, P. W. Gout, L. Morganti, *J. Chromatogr. A* **2003**, 988, 1.
- [41] S. Carter, S. Rimmer, R. Rutkaite, L. Swanson, J. P. A. Fairclough, A. Sturdy, M. Webb, *Biomacromolecules* **2006**, 7, 1124.
- [42] B. Mattiasson, A. Kumar, A. E. Ivanov, I. Y. Galaev, *Nat. Protocols* **2007**, 2, 213.
- [43] C. Hart, B. Schulenberg, Z. Diwu, W.-Y. Leung, W. F. Patton, *Electrophoresis* **2003**, 24, 599.
- [44] G. B. Sigal, C. Bamdad, A. Barberis, J. Strominger, G. M. Whitesides, *Anal. Chem.* **1996**, 68, 490.
- [45] L. Schmitt, C. Dietrich, R. Tampe, *J. Am. Chem. Soc.* **1994**, 116, 8485.
- [46] I. T. Dorn, K. R. Neumaier, R. Tampe, *J. Am. Chem. Soc.* **1998**, 120, 2753.
- [47] H. Y. Cho, M. A. Kadir, B.-S. Kim, H. S. Han, S. Nagasundarapandian, Y.-R. Kim, S. B. Ko, S.-G. Lee, H.-j. Paik, *Macromolecules* **2011**, 44, 4672.
- [48] Y.-Y. Luk, M. L. Tingey, D. J. Hall, B. A. Israel, C. J. Murphy, P. J. Bertics, N. L. Abbott, *Langmuir* **2003**, 19, 1671.
- [49] S.-Y. Kim, N. Ayyadurai, M.-A. Heo, S. Park, Y. J. Jeong, S.-G. Lee, *J. Microbiol. Biotechnol.* **2009**, 19, 72.